IEEE Access
Multidisciplinary ⋮ Rapid Review ⋮ Open Access Journal

Received 18 October 2024, accepted 27 October 2024, date of publication 4 November 2024, date of current version 13 November 2024.

Digital Object Identifier 10.1109/ACCESS.2024.3489646

RESEARCH ARTICLE

Development of a Balanced-to-Balanced Filtering Power Divider Based on Right-Angled Isosceles Triangular Patch Resonator

XUANQI LV[1], YIRU BIAN[1], YIJIE HUANG[2], YIXING LU[1], AND JIANPENG WANG[1], (Member, IEEE)

[1]School of Electronic and Optical Engineering, Nanjing University of Science and Technology, Nanjing 210094, China
[2]Qian Xuesen College, Nanjing University of Science and Technology, Nanjing 210094, China

Corresponding author: Jianpeng Wang (eejpwang@njust.edu.cn)

This work was supported in part by the College Students Innovation and Entrepreneurship Training Program of Nanjing University of Science and Technology.

ABSTRACT In this paper, a new design for balanced-to-balanced (BTB) filtering power divider (FPD) is proposed. Originating from the electric field distribution property of TM_{30} resonant mode on the right-angled isosceles triangular patch resonator (RAITPR), the feasibility of balanced-to-balanced power division is initially established. Afterwards, redundant modes suppression performance is achieved by loading metallic via holes on the RAITPR. Besides, by etching an L-shaped slot on the RAITPR an extra transmission zero has been introduced outside the differential mode (DM) passband. As such, the prototype of the BTB FPD has been well developed based on a single resonator. Ultimately, to verify this design concept, a BTB FPD demonstrator at the central frequency of 2.48 GHz is designed and fabricated. Both the simulated and the measured results are provided in good accordance. Within the passband, the minimum measured insertion loss of the BTB FPD is 1.18 dB and its 3-dB fractional bandwidth (FBW) reaches 24.2%. While outside the passband, both lower and higher order resonant modes of the RAITPR up to 4.0 GHz have been suppressed as expected.

INDEX TERMS Balanced-to-balanced (BTB), filtering power divider (FPD), L-shaped slot, right-angled isosceles triangular patch resonator (RAITPR).

I. INTRODUCTION

Power dividers are indispensable components that facilitate efficient power distribution, enabling seamless integration and performance optimization within radio frequency (RF) front-end systems. Recently, research on functionally integrated power dividers has received increasing attention owing to their extensive utilization within antenna feed networks and related areas. To date, numerous studies have been conducted on filtering power dividers (FPDs) [1], [2], [3], multi-way FPDs [4], [5], [6], quadrature/anti-phase power dividers [7], [8], unbalanced-to-balanced power dividers [9], [10], [11], [12] and so on.

On the other side, balanced-to-balanced (BTB) circuits have demonstrated immense potential as their immunity against environmental noises and electromagnetic interferences [13], [14], [15]. Accordingly, the BTB power divider and FPD have also been extensively studied [16], [17], [18], [19], [20], [21], [22]. In [16], a BTB power divider is designed. It combines a Wilkinson power divider with a balun structure by using a double-layer PCB structure, which increases the complexity of the structural design and the difficulty of practical application. By combining the half-wavelength resonator and the short-circuit branch loaded resonator, a BTB FPD is proposed in [17]. Although this method can realize a compact structure and good common mode rejection, its design complexity and insertion loss are increased owing to the side coupling structure between multiple resonators. By virtue of the resonant

The associate editor coordinating the review of this manuscript and approving it for publication was Li Yang.

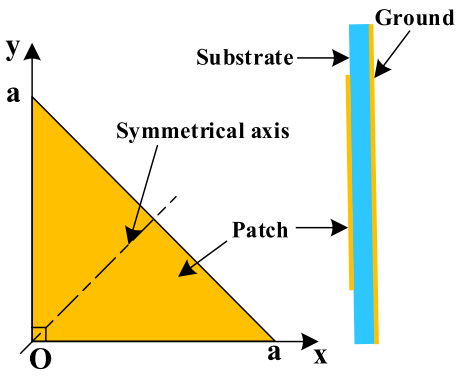

FIGURE 1. Structure of a RAITPR.

properties of the TE_{m0n} modes in the cavity structure, a substrate integrated waveguide (SIW) BTB FPD has been excogitated in [18]. Despite the advantage of high power capacity, this scheme confronts with the challenges of bulky volume and large phase deviation between the output ports. Furthermore, by introducing multiple resonant modes of cylindrical dielectric resonators into a metal cavity, a BTB FPD with high power capacity is also designed in [19]. However, due to the three-dimensional cavity structure form, the factors of volume and weight limit its application in balanced feed networks of low-profile antenna arrays.

The main purpose of this paper is to present a new BTB FPD based on a single-layer RAITPR. Originating from the analysis of electric field distribution of resonant modes on the RAITPR, the feasibility of balanced-to-balanced power division is established by virtue of the TM_{30} mode. Then, the RAITPR is evolved by wisely loading metallic via holes at designated positions. Attributing to the specific boundary conditions of the modified RAITPR, the proposed resonator can keep TM_{30} mode, while suppressing other redundant modes. Besides, due to the introduction of an L-shaped slot, the proposed design achieves good frequency selection characteristics for differential mode (DM) signals. Both simulated and measured results of the implemented BTB FPD are found in good agreement and demonstrate the advantages of low insertion loss, broad operating bandwidth and good filtering selectivity.

II. PRINCIPLE, GEOMETRY, AND ANALYSIS

A. ELECTRIC FIELD DISTRIBUTIONS OF RESONANT MODES ON RAITPR

Fig. 1 indicates the layout of a RAITPR, where a right-angled isosceles triangular patch is implemented on a single-layer dielectric substrate with a ground plane. To better analyze this resonator, the electric field of TM_{mn} mode on this resonator can be represented by the following formula [23].

$$E_z(x,y) = A_{m,n}(\cos\frac{m\pi x}{a}\cos\frac{n\pi x}{a} + (-1)^{m+n}cos\frac{n\pi x}{a}\cos\frac{m\pi x}{a})$$

$$H_x = \frac{j}{\omega\mu_0}\frac{\partial E_z}{\partial y}$$
$$H_y = \frac{-j}{\omega\mu_0}\frac{\partial E_z}{\partial x} \quad (1)$$

Besides, the corresponding resonant frequency can be expressed as

$$f_{mn} = \frac{c}{2a\sqrt{\varepsilon_r}}\sqrt{m^2+n^2} \quad (2)$$

where m and n are the two non-negative integers, a is the length of the right side of the RATPR and c is the light speed in free space.

According to (1), the corresponding normalized electric field equipotential line patterns of the first six modes on a RAITPR are depicted in Fig. 2. Specifically, Fig. 2(f) gives the normalized electric field equipotential line of the utilized TM_{30} mode. It is worth noting that the electric field at symmetric location with respect to the symmetric axis has the same magnitude and opposite direction which means balanced signals can be well excited and transmission in an equal-split power division form under this mode on the resonator. Specifically, when differential excitation is imposed on the resonator at symmetrical positions of 1^+ and 1^-, 2^+ and 2^-, as well as their symmetric locations 3^- and 3^+, receive differential signals with equal energy. This design method capitalizes on the intrinsic symmetry exhibited by the resonator's response to differential excitation, thereby achieving a balanced power distribution among the output differential ports.

Besides, since redundant modes in Fig. 2(a-e) are not desired in design, the suppression of these modes has also been taken into consideration. It can be divided into two steps. On the first step, the above-mentioned excitation method of differential signals breaks the symmetry of the modes in Fig. 2 (b), (c), and (e), thus these modes cannot be excited. On the second step, an artificial electric wall can be further constructed without affecting the TM_{30} mode by loading metallic via holes in the position shown in Fig. 2 (f). As such, this electric wall at specific location will inhibit TM_{10} and TM_{21} modes in Fig. 2 (a) and (d).

B. DEVELOPMENT OF THE BTB FPD

According the analysis mentioned above, a prototype of BTB FPD at the center frequency of 2.48 GHz is developed in Fig. 3(a). The balanced input port 1 is formed by microstrip lines 1a and 1b, while the balanced output port 2 and 3 are respectively formed by microstrip lines 2a and 2b as well as 3a and 3b. It should be mentioned that the positions of these feeding lines are determined by the analysis results of the electric field in Fig. 2(f). Besides, to achieve effective isolation between the balanced output ports 2 and 3, isolation resistors are introduced between the in-phase ports 2a and 3a, as well as 2b and 3b. Specifically, the grooves etched on the ground plane, in conjunction with the signal lines within them, form a coplanar waveguide (CPW) transmission line structure. The CPW transmission lines are interconnected

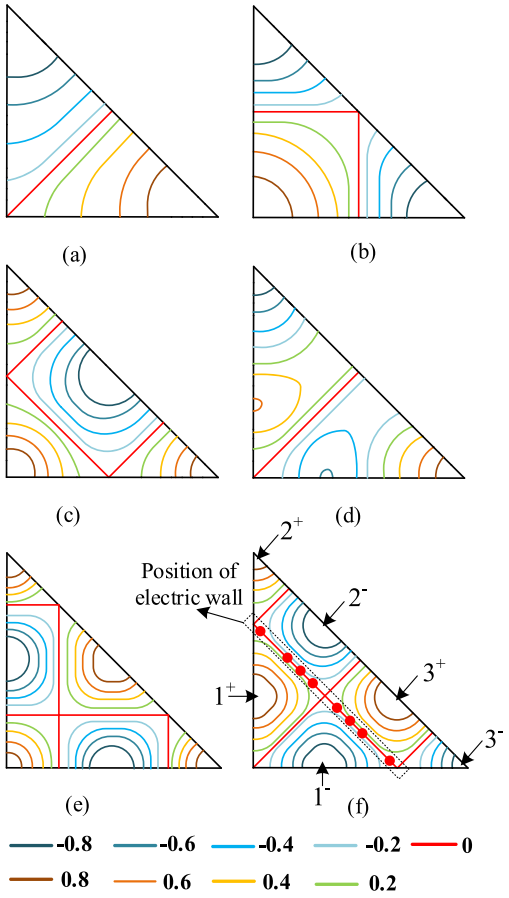

FIGURE 2. Normalized electric field equipotential line patterns on RAITPR. (a) TM_{10}. (b) TM_{11}. (c) TM_{20}. (d) TM_{21}. (e) TM_{22}. (f) TM_{30}.

with the microstrip lines located on the upper surface of the dielectric substrate through metallic via holes, thereby constituting two bridge-like structures, each of them spans across the microstrip lines 2b and 3a respectively. Afterwards, the developed bridge structures are connected to resistors through the microstrip lines, resulting in the parallel insertion of resistors between pairs 2a and 3a, as well as between 2b and 3a.

Simulated by ANSYS HFSS, Fig. 3(b) demonstrates the input reflection coefficients with and without metallic via holes when 1a and 1b are excited under differential signals. As for the metallic via holes arranged along a straight line form, they aim to construct an equivalent electrical wall at the corresponding position where electric field equals to zero in Fig. 2(f). The developed scheme can not only suppress the redundant modes mentioned above, but also be effective for the higher-order modes to some extent. In addition, considering that a single resonator with a fixed structure is utilized, the bandwidth of the proposed prototype circuit is mainly determined by the external quality factor Q_e. Thus, changing the position of feeding ports, which is represented by l in Fig. 3(a), different values of Q_e will be realized so as to vary the bandwidth of the BTB FPD. As can be seen in Fig. 3(c), the working bandwidth can be enhanced

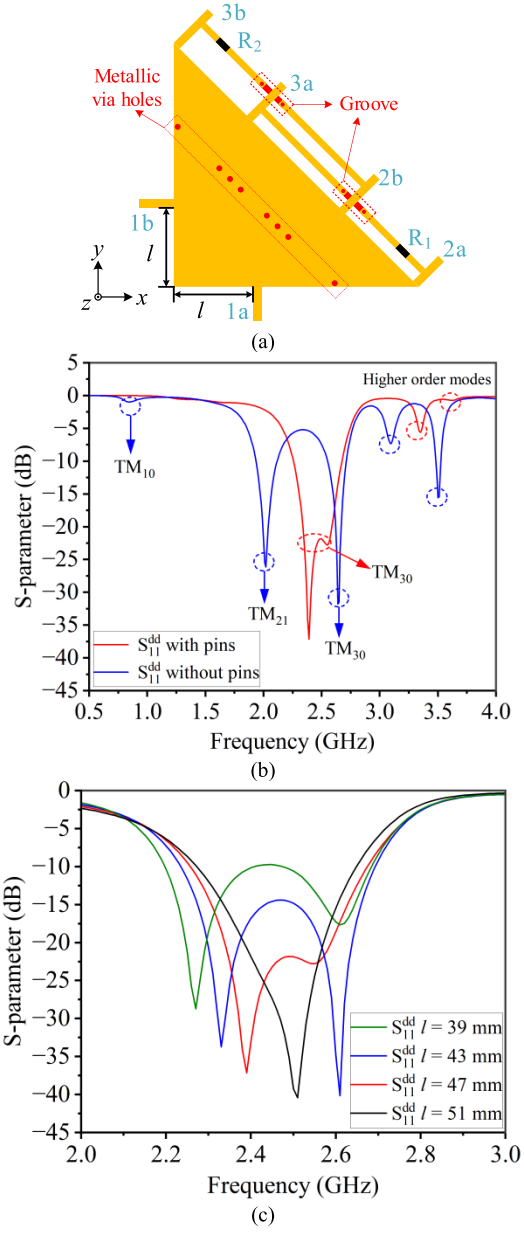

FIGURE 3. (a) The prototype circuit. (b) Reflection coefficients with and without metallic via holes. (c) Reflection coefficients versus the changing of *l*.

with the decreasing of l. Moreover, to improve the frequency selectivity, two transmission zeros occurring at 3.09 and 3.44 GHz are respectively introduced in the upper stopband. For the first transmission zero, i.e., at 3.09 GHz, it might be generated by the resonance on the isolation network in Fig. 4. As shown in Fig. 5 (a), the distribution of electric field is mainly concentrated on the isolated network. As for the second transmission zero, i.e., at 3.44 GHz, it is caused by the resonance of the square patch, which is separated from the original RAITPR by the slot structure in Fig. 4. Since the slot structure is located in accordance with the gradient direction along the electric field equipotential lines of TM_{30} mode, it will keep the transmission performance

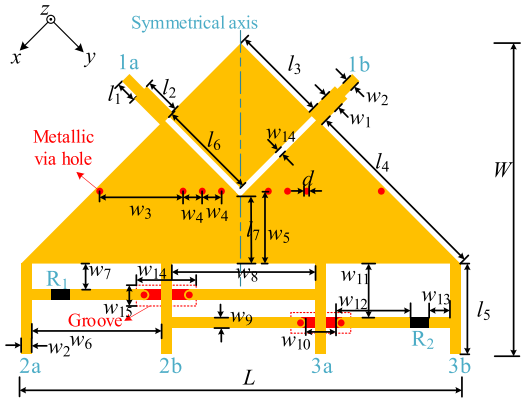

FIGURE 4. Circuit layout and detailed dimensions of the proposed BTB FPD ($l_1 = 5$, $l_2 = 16$, $l_3 = 27$, $l_4 = 62.5$, $l_5 = 19$, $l_6 = 28.4$, $l_7 = 25$, $w_1 = 3.6$, $w_2 = 1.2$, $w_3 = 22$, $w_4 = 7$, $w_5 = 22$, $w_6 = 41.6$, $w_7 = 10.2$, $w_8 = 42.7$, $w_9 = 0.8$, $w_{10} = 3.2$, $w_{11} = 11.6$, $w_{12} = 31.1$, $w_{13} = 7.6$, $w_{14} = 6$, $w_{15} = 2$, $d = 0.5$, $L = 131$, $W = 85$, all in millimeters, Resistor $R_1 = R_2 = 120$ Ohm).

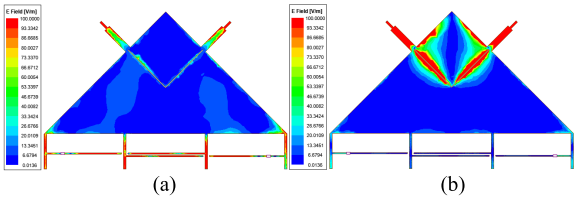

FIGURE 5. Intensity diagram of electric field at (a) 3.09 GHz and (b) 3.44 GHz.

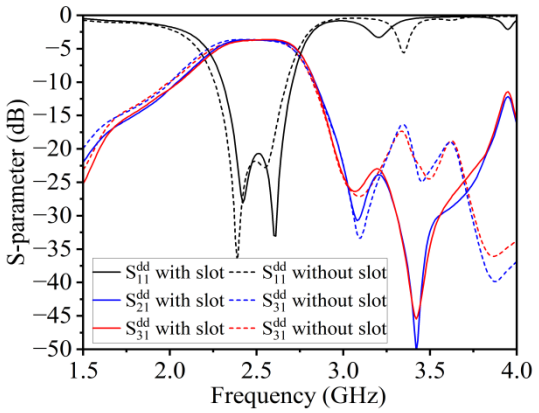

FIGURE 6. DM responses with and without the L-shaped slot.

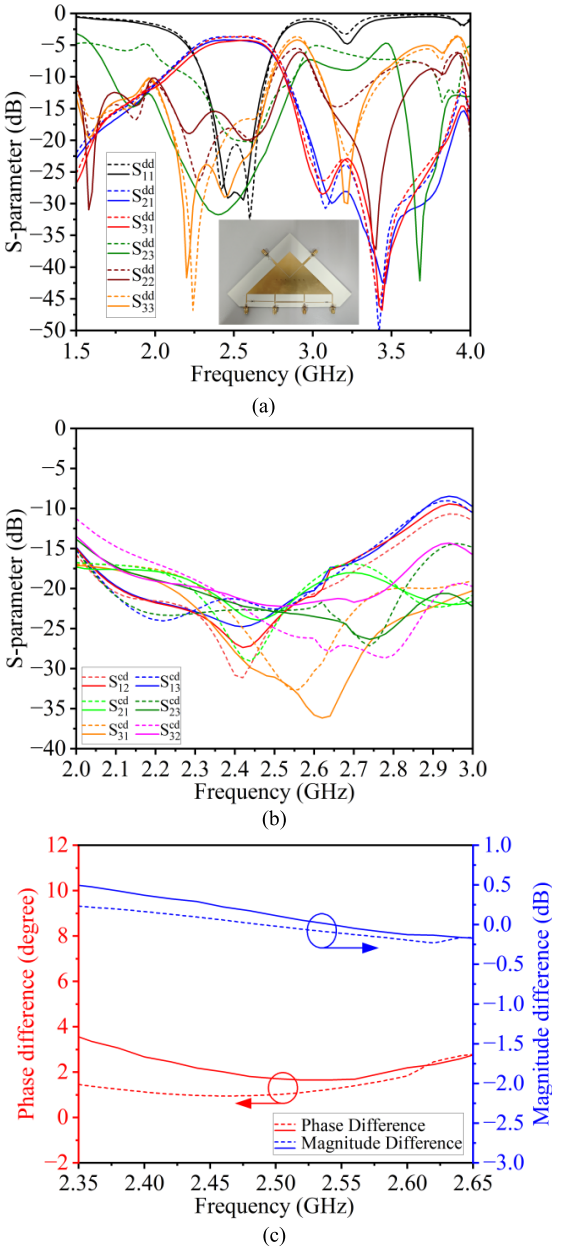

FIGURE 7. Simulated (dashed lines) and measured (solid lines) performance of the proposed BTB FPD. (a) and (b) S-parameters. (c) Imbalance of phase and amplitude.

basically unchanged within the passband. While at the specific resonant frequency of 3.44 GHz of the separated square patch, the electric field is mainly concentrated on the square patch resonator as demonstrated in Fig. 5(b). Under this circumstance, a coupling topology of extracted-zero has been formed, thus introducing an extra transmission zero at upper stopband. For validation, the DM responses of the BTB FPD with and without L-shaped slot are given in Fig. 6. As expected, an extra transmission zero is successfully introduced by the adoption of the L-shaped slot.

III. IMPLEMENTATION AND RESULTS

To verify the feasibility of the proposed design method, one demonstrator BTB FPD was implemented on the Rogers 4350 substrate with a permittivity of 3.66, and a loss tangent of 0.004. Simulated and measured results are shown in Fig. 7. As the measured results depict, for DM signals, the BTB FPD operates at the center frequency of 2.48 GHz with a 3-dB FBW of 24.2% (2.18-2.78 GHz). Good matching is achieved during the operating band of 2.35-2.65 GHz with a maximum return loss of -15 dB. The measured in-band minimum insertion loss is 1.18 dB for Sdd 21 and 1.25 dB for Sdd 31 while the simulated results are 0.63 dB and 0.71 dB respectively. Besides, both measured Sdd 21 and Sdd 31 are less than -20 dB during the band of 2.98-3.85 GHz and the suppression reaches -40 dB during the band of

TABLE 1. Comparison with other reported BTB FPDs.

References	f_0 (GHz)	3-dB FBW(%)	IL (dB)	Iso. (dB)	DM SF of -20 dB	Num. of RESs	Type of RESs	Size ($\lambda_g \times \lambda_g$)
[17]	2.39	7	2.21	20	3.89	4	Microstrip	0.46×0.4
[18]	28&39	3.6/3.1	1.4/1.9	13/13	2.61/1.92	3	SIW	3.0×2.1
Design I in [21]	1.8	18.2	1.08	29.5	2.29	2	Patch	0.55×0.55
Design II in [21]	1.8	11.7	1.02	32.1	2.85	2	Patch	0.55×0.55
[22]	14.91	4.1	1.3	16.1	4.83	4	SIW	0.59×0.71
This work	**2.48**	**24.2**	**1.18**	**24**	**2.2**	**1**	**Patch**	**1.83×1.19**

FBW: fractional bandwidth, f_0: central frequency, IL: insertion loss, Iso.: isolation, SF of -20dB: the shape factor of -20 dB (FBW of 20-dB/FBW of 3-dB), Num.: number, RESs: resonators.

3.42-3.47 GHz. Fig. 7(b) indicates the CM performance of the BTB FPD and the imbalance information between the two output ports is demonstrated in Fig. 7(c). As can be seen from Fig. 7(c), within the operating band the measured magnitude difference is less than 0.5 dB and the phase difference is less than 3.5 degree. Table 1 lists the relevant works on BTB PFDs. Compared with designs I and II in [21], our work achieves a wide operating bandwidth. With regarding to works in [17] [18] and [22], our design exhibits advantages in both insertion loss, and operating bandwidth. In addition, excellent selectivity is achieved with only one single patch resonator, which demonstrates the low complexity in our design.

IV. CONCLUSION

A new BTB FPD based on a single-layer RAITPR is presented in this article. By analyzing the electric field distribution of resonant modes on the RAITPR, the principle of balanced-to-balanced power division is illustrated by utilizing the TM_{30} resonant mode. Then, to suppress other redundant modes while keeping the operation mode, the RAITPR is modified by wisely loading metallic via holes at specific positions. Afterwards, to improve the frequency selectivity for DM signals, an L-shaped slot is further introduced into the RAITPR so as to realize an extra transmission zero at upper stopband. Both simulated and measured results are provided in good accordance and demonstrate the developed BTB FPD has the advantages of low insertion loss, wide operating bandwidth and excellent filtering characteristics.

REFERENCES

[1] J.-X. Chen, Y. Xue, X. Shi, Y.-X. Huang, W. Qin, and Y.-J. Yang, "Design of double-ridge waveguide balanced filter and filtering power divider," *IEEE Trans. Microw. Theory Techn.*, vol. 72, no. 10, pp. 5929–5937, Oct. 2024, doi: 10.1109/TMTT.2024.3386731.

[2] X.-L. Zhao, L. Gao, X. Y. Zhang, and J.-X. Xu, "Novel filtering power divider with wide stopband using discriminating coupling," *IEEE Microw. Wireless Compon. Lett.*, vol. 26, no. 8, pp. 580–582, Aug. 2016.

[3] Y. Deng, J. Wang, L. Zhu, and W. Wu, "Filtering power divider with good isolation performance and harmonic suppression," *IEEE Microw. Wireless Compon. Lett.*, vol. 26, no. 12, pp. 984–986, Dec. 2016.

[4] F.-J. Chen, L.-S. Wu, L.-F. Qiu, and J.-F. Mao, "A four-way microstrip filtering power divider with frequency-dependent couplings," *IEEE Trans. Microw. Theory Techn.*, vol. 63, no. 10, pp. 3494–3504, Oct. 2015.

[5] H.-Y. Li, J.-X. Xu, Y. Yang, and X. Y. Zhang, "Novel switchable filtering circuit with function reconfigurability between SPQT filtering switch and four-way filtering power divider," *IEEE Trans. Microw. Theory Techn.*, vol. 68, no. 3, pp. 867–876, Mar. 2020.

[6] G. Zhang, Y. Liu, E. Wang, and J. Yang, "Multilayer packaging SIW three-way filtering power divider with adjustable power division," *IEEE Trans. Circuits Syst. II, Exp. Briefs*, vol. 67, no. 12, pp. 3003–3007, Dec. 2020.

[7] Z. Xia, J. Wang, Q.-Y. Lu, W. Wu, and J. Hong, "A wideband 90° phase shifting element applied in quadrature phase filtering power divider," *IEEE Microw. Wireless Technol. Lett.*, vol. 34, no. 2, pp. 167–170, Feb. 2024.

[8] P. Zhao, Q. Wang, X. Tian, and X. Wang, "An integratable planar waveguide power divider with anti-phases and full bandwidth," *IEEE Microw. Wireless Compon. Lett.*, vol. 26, no. 8, pp. 583–585, Aug. 2016.

[9] Z. Xia, J. Wang, Q.-Y. Lu, W. Wu, and J. Hong, "Development of an unbalanced-to-balanced filtering power divider with sequential rotation phase characteristic," *IEEE Microw. Wireless Technol. Lett.*, vol. 34, no. 1, pp. 21–24, Jan. 2024.

[10] Y. Wu, Z. Zhuang, M. Kong, L. Jiao, Y. Liu, and A. A. Kishk, "Wideband filtering unbalanced-to-balanced independent impedance-transforming power divider with arbitrary power ratio," *IEEE Trans. Microw. Theory Techn.*, vol. 66, no. 10, pp. 4482–4496, Oct. 2018.

[11] X. Gao, W. Feng, W. Che, and Q. Xue, "Wideband balanced-to-unbalanced filtering power dividers based on coupled lines," *IEEE Trans. Microw. Theory Techn.*, vol. 65, no. 1, pp. 86–95, Jan. 2017.

[12] W. Zhang, Y. Wu, Y. Liu, F. M. Ghannouchi, and A. Hasan, "A wideband balanced-to-unbalanced coupled-line power divider," *IEEE Microw. Wireless Compon. Lett.*, vol. 26, no. 6, pp. 410–412, Jun. 2016.

[13] H. Tian, H. Liu, and Z. Song, "Miniaturized highly selective balanced ultrawideband HTS bandpass filter using CRLH transmission line aided by gray wolf algorithm," *IEEE Microw. Wireless Technol. Lett.*, vol. 33, no. 12, pp. 1607–1610, Dec. 2023.

[14] X.-B. Zhao, F. Wei, L. Yang, and R. Gómez-García, "Two-layer-magic-T-based bandpass, quasi-bandstop, and dual-passband balanced filters with differential-/common-mode reflectionless behavior," *IEEE Trans. Microw. Theory Techn.*, vol. 72, no. 4, pp. 2267–2282, Apr. 2024.

[15] X.-B. Zhao, F. Wei, P. F. Zhang, and X. W. Shi, "Mixed-mode magic-ts and their applications on the designs of dual-band balanced out-of-phase filtering power dividers," *IEEE Trans. Microw. Theory Techn.*, vol. 71, no. 9, pp. 3896–3905, Sep. 2023.

[16] J. Shi, J. Wang, K. Xu, J.-X. Chen, and W. Liu, "A balanced-to-balanced power divider with wide bandwidth," *IEEE Microw. Wireless Compon. Lett.*, vol. 25, no. 9, pp. 573–575, Sep. 2015.

[17] M. Luo, X. Xu, X.-H. Tang, and Y.-H. Zhang, "A compact balanced-to-balanced filtering Gysel power divider using $\lambda_g/2$ resonators and short-stub-loaded resonator," *IEEE Microw. Wireless Compon. Lett.*, vol. 27, no. 7, pp. 645–647, Jul. 2017.

[18] P.-L. Chi, Y.-M. Chen, and T. Yang, "Single-layer dual-band balanced substrate- integrated waveguide filtering power divider for 5G millimeter-wave applications," *IEEE Microw. Wireless Compon. Lett.*, vol. 30, no. 6, pp. 585–588, Jun. 2020.

[19] H.-Y. Li, J.-X. Xu, and X. Y. Zhang, "Miniaturized balanced filtering power dividers with arbitrary power division ratio using multimode dielectric resonator in single cavity," *IEEE Trans. Circuits Syst. II, Exp. Briefs*, vol. 69, no. 6, pp. 2707–2711, Jun. 2022.
[20] G. Zhang, Q. Zhang, Q. Liu, W. Tang, and J. Yang, "Design of a new dual-band balanced-to-balanced filtering power divider based on the circular microstrip patch resonator," *IEEE Trans. Circuits Syst. II, Exp. Briefs*, vol. 68, no. 12, pp. 3542–3546, Dec. 2021.
[21] Q. Liu, J. Wang, L. Zhu, G. Zhang, and W. Wu, "Design of a new balanced-to-balanced filtering power divider based on square patch resonator," *IEEE Trans. Microw. Theory Techn.*, vol. 66, no. 12, pp. 5280–5289, Dec. 2018.
[22] J. Zheng, X. Zhou, W. Tang, Y. Liu, G. Zhang, H. Yang, and J. Yang, "Design of balanced to balanced filtering power divider based on right triangle substrate integrated waveguide cavity," *Int. J. RF Microw. Comput.-Aided Eng.*, vol. 31, no. 9, Sep. 2021, Art. no. e22766.
[23] R. Chadha and K. C. Gupta, "Green's functions for triangular segments in planar microwave circuits," *IEEE Trans. Microw. Theory Techn.*, vol. MTT-28, no. 10, pp. 1139–1143, Oct. 1980.

XUANQI LV was born in Taizhou, Jiangsu, China, in 2003. He is currently pursuing the bachelor's degree with Nanjing University of Science and Technology.

He majored in radar in electronic information engineering.

YIRU BIAN was born in Yangzhou, Jiangsu, China. He received the B.S. degree from Nantong University, Nantong, China, in 2021. He is currently pursuing the Ph.D. degree in electronic science and technology with Nanjing University of Science and Technology, Nanjing.

His current research interests include wireless power transmission and GaAs-based MMIC.

YIJIE HUANG was born in Wuxi, Jiangsu, China, in 2002. He is currently pursuing the B.S. degree in electronic information engineering with Nanjing University of Science and Technology, Nanjing, China.

His current research interest includes microwave antennae.

YIXING LU was born in Huludao, Liaoning, China, in 2002. He is currently a Senior with Nanjing University of Science and Technology, Nanjing, Jiangsu, China. His major is optoelectronic information science and engineering.

JIANPENG WANG (Member, IEEE) received the Ph.D. degree from the University of Electronic Science and Technology of China, Chengdu, China, in 2007.

From 2005 to 2006, he was a Research Assistant with the Institute for Infocomm Research, Singapore. From 2010 to 2011, he was a Research Fellow with the School of Electrical and Electronic Engineering, Nanyang Technological University, Singapore. In 2013, he joined the School of Engineering and Physical Sciences, Heriot-Watt University, Edinburgh, U.K., as a Visiting Scholar. From 2014 to 2016, he was a Research Fellow with the Faculty of Science and Technology, University of Macau, Macau, China. He is currently a Professor with the School of Electronic and Optical Engineering, Nanjing University of Science and Technology, Nanjing, China. He has authored or co-authored more than 120 articles in international journals and conference proceedings. His current research interests include microwave circuits, antennas, and low-temperature co-fired ceramic (LTCC)-based millimeter-wave circuits.

Dr. Wang was an Associate Editor of *IET Electronics Letters*, from 2015 to 2018.